Journal of Instrumentation

SISSA

OPEN ACCESS

In situ micro gas tungsten constricted arc welding of ultra-thin walled 2.275 mm outer diameter grade 2 commercially pure titanium tubing

To cite this article: L. Cooper *et al* 2020 *JINST* **15** P06022

Published by IOP Publishing for Sissa Medialab
Received: *February 2, 2020*
Accepted: *April 30, 2020*
Published: *June 17, 2020*

In situ micro gas tungsten constricted arc welding of ultra-thin walled 2.275 mm outer diameter grade 2 commercially pure titanium tubing

L. Cooper,[a] **M. Crouvizier,**[b] **S. Edwards,**[c] **R. French,**[c] **F. Gannaway,**[d] **P. Kemp-Russell,**[c] **H. Marin-Reyes,**[c] **I. Mercer,**[e] **A. Rendell-Read,**[f] **G. Viehhauser**[g] **and W. Yeadon**[c,1]

[a] *Rutherford Appleton Laboratory, Science and Technology Facilities Council, Harwell Science and Innovation Campus, Didcot, OX11 0QX, United Kingdom*
[b] *Mechanical and Materials Engineering, CERN, Geneva, 1211, Switzerland*
[c] *Department of Physics and Astronomy, The University of Sheffield, Sheffield, South Yorkshire, S10 2TN, United Kingdom*
[d] *School of Physics and Astronomy, Queen Mary, University of London, London, E1 4NS, United Kingdom*
[e] *Physics Department, Lancaster University, Lancaster, Lancashire, LA1 4YW, United Kingdom*
[f] *VBC Instrument Engineering ltd., Wellingborough, Northamptonshire, NN8 6GR, United Kingdom*
[g] *Department of Physics, University of Oxford, Oxford, Oxfordshire, OX1 4BH, United Kingdom*

E-mail: will.yeadon@sheffield.ac.uk

Abstract: Ultra-thin walled cooling tubes for heat exchangers and condenser units have applications in multiple high-value manufacturing industries. Grade 2 commercially pure titanium (CP-2 Ti) requires far less mass to achieve the same mass flow handling abilities as stainless steel tubing yet it is more challenging to join, particularly at wall thicknesses less than 500 µm (termed ultra-thin walled tube). This paper presents a single-pass joinery method that produces reliable welds on 2.275 mm outer diameter (OD), 160 ± 10 µm wall thickness tubing with a service life of 20 of more years. This is achieved through an automated orbital gas tungsten constricted arc welding (GTCAW) process incorporating enveloping low-mass sleeves used in tandem with a buttressing internal gas pressure to support the molten metal and maintain consistent internal diameter inside the tube. The industrial applicability is demonstrated through the production of a 1:1 scale mock-up of a fixed geometry CO_2 cooling circuit for a next-generation particle detector. The tensile strengths of the joints, 403.8 ± 4.2 MPa, exceed the tensile strength of the parent CP-2 Ti.

Keywords: Detector design and construction technologies and materials; Manufacturing; Detector cooling and thermo-stabilization

[1] Corresponding author.

https://doi.org/10.1088/1748-0221/15/06/P06022

2020 JINST 15 P06022

Contents

2020 JINST 15 P06022

1 Introduction

A common application of thin-walled titanium tubing is in condenser units, where the wall thickness of these tubes are rarely below 500 µm. Yet, there are applications, like cooling circuits in next-generation particle physics experiments, which necessitate wall thicknesses below conventional industrial limits. The ATLAS detector at the CERN Large Hadron Collider [1] is coming to the end of its service life. To facilitate investigations into higher centre of mass energy levels probing for new physics, the ATLAS detector is being upgraded [2]. Working at the core of the proposed upgraded ATLAS detector is the ITk, the replacement for the current ATLAS Inner Detector. The ITk will have an all-silicon semiconductor tracking system consisting of an inner 5-layer pixel detector surrounded by a 4-layer strip detector. The ITk Strip Detector [3] has small read-out electronics built into staves for the cylindrical portion of the detector and into petals for the disk portion. To remove the heat load from these detector electronics, the ITk Strip Detector stave design has an embedded titanium cooling circuit within its carbon fibre structure. The cooling circuits in the stave design feature 2.275 mm outer diameter (OD), 160 µm wall thickness, grade 2 commercially

pure titanium (CP-2 Ti) tubing. This commercially pure titanium tubing provides a 42% weight saving compared to stainless steel tubing with the same mass flow handling ability. Despite the attractive properties of titanium (high strength to weight ratio and excellent corrosion resistance), welding challenges have encumbered its industrial application in thin-walled tubing. Specifically, as welding procedures do not scale down proportionally and titanium is relatively more difficult to join compared to other metals, thin-walled tube welding is particularly challenging. ASTM standard B862 [4, 5] for welding Titanium Pipe stops above 1000 µm in wall thickness and 10 mm in outer diameter and the granularity for outer diameter tolerance in titanium condenser and heat exchanger tubes in ASTM standard B338 [6] stops at 25.4 mm. Thus, welding the thin-walled CP-2 Ti tubing for the ATLAS ITk Strip Detector Stave cooling circuits requires a custom welding procedure. The most popular and reliable thin sheet and thin-walled tube welding methods for titanium include Electron Beam Welding (EBW), Laser Beam Welding (LBW) and variations of Gas Tungsten Arc Welding (GTAW). Comparatively, EBW and LBW offer better weld properties in some circumstances than GTAW [7], however, they lack the advantage of in situ operation available to GTAW. Specifically, the equipment to create a high vacuum for EBW and the bulky equipment required for LBW could not physically fit into smaller areas for in situ production. In situ production is a critical requirement for the ATLAS ITk cooling system eliminating LBW and EBW as candidates. Further, GTAW based welding is considerably cheaper than EBW or LBW. GTAW produces precise, clean and strong joints on titanium and it is the industry standard for titanium joinery.

Gas Tungsten Constricted Arc Welding (GTCAW) is a variant of GTAW where the arc width is reduced through high frequency pulsing of the welding current. GTCAW focuses the heat input and reduces the heat affected zone (HAZ) of the produced weld. This concentration of the heat flow enables the successful production of welds on conventionally challenging welding jobs such as orbital welding of thin-walled tubing. The heat flow during orbital tube welding of thin-walled tubing is different to the heat flow during thin sheet welding. This is because in orbital welding the direction of the maximum temperature gradient is continuously changing as the heat source revolves around the tube. Thus, the thermal gradients are shallower and the cooling rate reduced in orbital welding compared to sheet welding. This complex heat flow limits the applicability of prior research into thin sheet welding to thin-walled tube welding.

Reports on thin-walled tube CP-2 joinery are very limited and, to the author's knowledge, only address wall thicknesses above 500 µm. de Garcia et al. [8] joined 6 mm OD, 1 mm wall thickness, CP-2 Ti tubing for a satellite propulsion system using orbital GTAW welding with internal pressurization to join the tubing. However, for alignment, they manually tacked the tubes together. The method detailed in the present work alleviates this requirement whilst also welding smaller OD and thinner walled tubes. There have been reports covering thin-walled CP-2 skelp production [9] and longitudinal welding of thin-walled CP-2 tubes [10]. However, these processes do not involve welding in a singular transverse plane thus the complex heat flow of orbital welding is not considered and these processes are more similar to thin sheet welding. However, for completeness, they are mentioned in the present work. Similarly, in tube-to-sheet welding or tube-to-end-fitting welding [11], the heat flow is again different resulting in a fundamentally different process.

Based on this literature survey, there is a paucity of academic research outlining the joinery of ultra-thin titanium tubing (where ultra-thin denotes a wall thickness of less than 500 µm).

2020 JINST 15 P06022

Initially, tests of commercial off-the-shelf technology for joinery of the 2.275 mm tube for the cooling system of the ATLAS ITk resulted in an excessive heat affected zone suggesting poor joint properties; this necessitated the development of a novel joinery method. Following several years of research and development in an Industry-Academia collaboration we developed a GTCAW technique (commercial name *InterPulse* see [12]) that, combined with buttressing internal gas flow, achieves satisfactory joinery of the thin-wall titanium tubing, see [13, 14]. However, the transfer from proof-of-concept to full production, including in situ operation, required considerable development and verification — particularly the understanding of equalizing the physical forces of the welding arc and the buttressing internal gas flow, as joints are often required several meters from the internal gas flow inlet.

The present work details the full production process for reliable, in situ, joinery on fixed orientation thin-walled titanium tubing used to make a demonstration two-phase CO_2 cooling plant for the ATLAS ITk, shown in figure 1. Further, an investigation of inner pressurization is undertaken with possible physical mechanisms suggested. Finally, the metallurgy of the produced joints is examined serving as qualification of the production process. Due to the complex challenges addressed, and the lack of literature on ultra-thin walled tube joinery, the present work provides an advance for next-generation cooling circuit and condenser tube production.

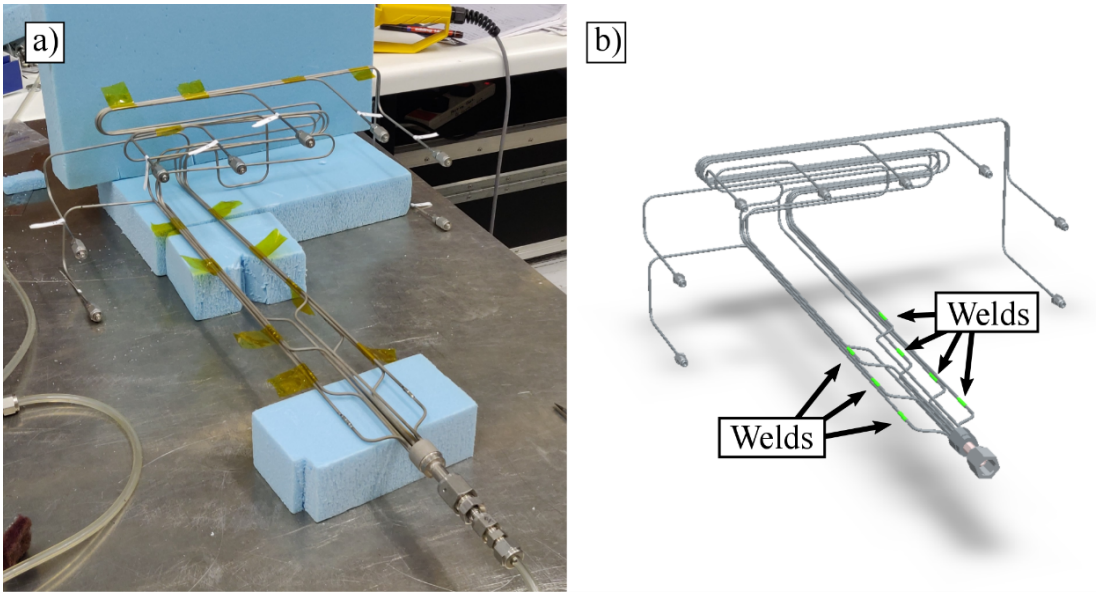

Figure 1. Produced part (a) and CAD model (b) of high-value cooling circuit for a two-phase CO_2 cooling plant. The joints are highlighted green in (b). The cooling plant will be used as a demonstration for the forthcoming ATLAS upgrade.

2 Past work on CP-2 titanium joinery

Commercially pure titanium grades are α alloys of titanium with oxygen and iron as their primary alloying elements. With a hexagonal close packed (HCP) α-phase and a body centred cubic (BCC) β-phase, CP-2 Ti is an α alloy that is moderately strong, corrosion resistant and has excellent

2020 JINST 15 P06022

cold forming properties. Protected by a TiO_2 film, usually between 50–200 Å thick, CP-2 Ti is approximately 99.6% pure titanium. Table 1 displays the ASTM composition requirements of CP-2 Ti. Joinery of CP-2 Ti is challenging principally due to embrittlement by hydrogen, nitrogen and oxygen absorption at the elevated temperatures of joinery (covered by [15]). Above 500°C, the oxidation resistance of titanium rapidly decreases allowing the aforementioned elements to dissolve interstitially creating microscopic hardening — increasing the cracking susceptibility of the titanium. Notably the HCP structure is unchanged with interstitial dissolution as the elements locate on interstitial sites within the crystal lattice. Processing CP-2 Ti above 875°C prompts the phase transformation of HCP α-phase to BCC β-phase; at these elevated temperatures CP-2 Ti experiences significant grain growth shown by [16]. The presence of iron as a significant impurity in CP-2 Ti lowers the beta transus starting temperature to 875°C as iron is a β phase stabiliser in CP-2 Ti. Whereas, the significant oxygen content serves as an α-phase stabilizer. In principle, most joinery techniques can be used with titanium. However, for reliability, in the present application, a welding technique was required and the GTAW process was judged the most apt.

Table 1. Chemical composition of CP-2 Ti.

Element	**C**	**N**	**O**	**H**	**Fe**	**Ti**
Weight %	≤ 0.08	≤ 0.03	≤ 0.25	≤ 0.015	≤ 0.30	Balance

Protecting titanium from embrittlement during welding has motivated considerable research on shielding gas supply; maintaining an inert atmosphere post weld is critical in preventing embrittlement. For the GTAW process, authors have broadly reported that the colour of the weld surface is a good indicator of weld contamination. Previous investigations into GTAW on CP titanium sheet report the benefits of three gas supply sources [17, 18] to shield the weld from impurities. Similarly, the use of custom gas delivery tooling [19] has been reported to produce good welds on CP titanium V grooved billets. These reports illustrate that sufficient shielding is vital in ensuring acceptable weld production on CP titanium. In the present work, following a consultation with industrial welding professionals, we apply substantial (20 seconds) enveloping pre-weld and post-weld shielding gas flow to enable acceptable weld production.

Cooling rate and formation of new structures are prominent factors influencing weld quality for titanium and its alloys as outlined by [20]. Cooling rates, between $90°Ks^{-1}$ to 600 Ks^{-1}, in CP-2 Ti promote massive transformation of β-bcc to α-hcp with the martensitic transformation beginning above $500°Ks^{-1}$ [21]. The $\alpha \rightarrow \beta \rightarrow \alpha$ transformation in welded CP-2 Ti exhibits strong texture memory as α-phase formations inherit their microstructure from β-phase grains during cooling [22]. Good quality welds should have granular-like grain morphologies promoted by lower cooling rates however, the inert atmosphere post-weld gas flow maintains has a cooling effect thus moderating its application is critical. Orbital welding produces a three-dimensional heat flow into the work piece resulting in complex multidirectional grain morphologies. Limiting the excessive grain growth at higher heat inputs is key in producing an integral weld. The ultra-thin walled tubes in the present work have limited neighbouring material thus the direction of the heat conduction is effectively limited to two dimensions. This exacerbates the grain growth with inputted heat. Thus, in the present work whilst substantial post-weld gas flow is applied, the flow rate is relatively low compared to typical GTAW flow rates.

2020 JINST 15 P06022

3 Joinery procedure

3.1 Gas Tungsten Constricted Arc Welding

Conventional GTAW or tungsten inert gas (TIG) welding is a fusion welding process involving the generation of an electric arc between a non-consumable Tungsten electrode and the work piece. Piped around the electrode, inert gas — typically argon or helium — shields the arc and weld pool during welding. The electric arc plasma is approximately a 50/50 mixture of ionized shielding gas and electrons. The movement of electrons and ionized shielding gas forms a current within the arc, Murphy [23] reported 80% of the heat input during GTAW is caused by this electrical current. Thus, of particular importance for GTAW when welding CP Ti is the significant drop in electrical resistivity with the phase transformation of $\alpha \rightarrow \beta$ at 875°C observed by [24]. This change in electrical resistivity enhances the heat input into the work piece.

Developed in the 1950s, pulsed current GTAW is a popular variant of GTAW where the current of the electric arc is pulsed between a higher peak current and a lower background current. Pulsed GTAW brings several advantages such as; enhanced arc stability, increased depth/width ratio and a narrower heat affected zone. Enhanced arc stability helps to reduce the chance of interruption of the welding process due to arc deflection. An increased weld depth/width ratio produces more integral joints, and a narrower heat affected zone limits the detrimental effects of heat on the work metal [25, 26]. In pulsed welding, authors have described a mechanism where the peak current provides more heat and increases the size of the weld pool whilst the background current maintains arc stability and provides a 'cooling period' for the metal to solidify producing a series of spot welds [27–30]. Whilst this may be correct for procedures using low pulsing rates and a large peak current to background current ratio, this description does not consider the response time of the arc plasma to an increase in the current control signal or the inertia of the arc plasma as the current magnitude changes. Thus, GTCAW requires a different description.

At very high pulsing rates, the arc is better understood as a stable 'mixed' state between the higher and lower current arcs. This description was first outlined by Saedi and Unkel [31] finding that at ~3 kHz the arc plasma did not change with the instantaneous current change. Furthermore, they found at current pulsing frequencies below 500 Hz the arcs did in fact respond to instantaneous changes in current validating the heating and cooling period description for pulsed GTAW. With the arc constriction understood as a mixed state, the physical phenomena behind the benefits of high pulsing rates are clear. Due to the Lorentz force, the current flow within the arc results in a radially inward 'pinch' effect with a force proportional to the square of the current (as both the current density and magnetic field in the arc are each dependent on the current). At the peak pulsing current the Lorentz force is quadratically increased but the response time of the arc plasma to the increase in current lags behind the increase in the Lorentz force. When the current subsequently decreases to the background level, the response of the arc plasma to the relaxation of the 'pinch' effect is again slower than the forthcoming increase back to the peak pulse level. Hence, the arc exists in a constricted 'mixed' state. The arc constriction focuses the conduction path between the electrode and work metal resulting in increased current density in the center of the arc compared to a conventional arc for the same current. Thus, less heat is 'wasted' in the arc plume and surrounding metal, and more is focused into the weld pool. This constriction has been well reported [32–34] and is the basis of the GTCAW process.

2020 JINST 15 P06022

The Interpulse system is a novel variant of GTCAW that employs a modulated current pulse waveform with a 20 kHz pulsing rate. In GTCAW, the shape of the current waveform (typically square-wave, saw tooth or sinusoidal current pulse shapes) influence the constriction of the GTCAW arc. The InterPulse system includes a modulated 20 kHz 'Delta current' that is superimposed on the peak and background currents altering the shape of the waveform. The high frequency pulsing combined with the atypical pulse waveform in the InterPulse system enables significant arc constriction focusing the heat input and reducing the HAZ. This HAZ reduction facilitates improved weld quality through dramatically reducing microfissuring and distortion in the wider work piece. An additional benefit to the significant arc constriction for CP-2 Ti welding is the reduced shielding gas required; as less metal is heated, less shielding gas is required to protect it from interstitial contaminant dissolution. The heat management benefits of the InterPulse arc are explored in detail in [12]. A visualization of arc constriction in the InterPulse system is shown in figure 2. In the present work, the InterPulse Arc is implemented in a specialized low-amperage welding machine, the VBCie IP50, to join the thin-walled titanium tube.

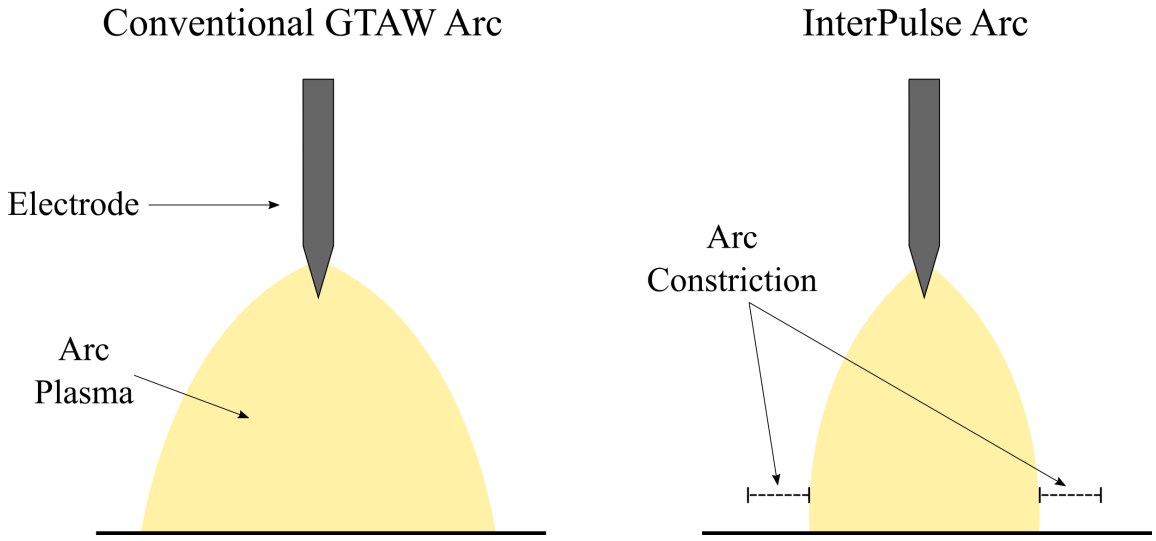

Figure 2. Comparison between a conventional GTAW arc and the InterPulse arc.

3.2 GTCAW application to thin-walled CP-2 titanium tubing

As outlined, the complex heat flow dynamic in orbital welding makes heat input control challenging. However, an additional challenge in orbital thin-walled tube welding is ensuring that the tube does not collapse under the pressure from the welding heat source. In the present work, maintaining a consistent inner diameter to ensure consistent mass flow throughout the cooling circuit is critical. Thus, during welding the interior of the tube is pressurized, termed inner diameter pressurization. Differing from conventional shielding to prevent oxidation when welding titanium, inner diameter pressurization provides a physical internal buttressing force for the molten metal during welding. To achieve this, two flows of shielding gas are used; an external shielding gas flow to prevent oxidation and an internal gas flow to both shield the metal and to provide inner diameter pressurization. Control over the buttressing support for the molten metal, sometimes several meters from the

2020 JINST 15 P06022

gas inlet, is achieved through tuning the gas inflow to produce a constant inner diameter in the welded tubes.

The typically imperfect ends of the ultra-thin walled cooling tubing often require rotation and reorientation to achieve complete face-to-face contact. This is unfeasible to perform in a fixed orientation in situ environment. We have therefore developed a custom enveloping fitting (figure 3) which facilitates exact positioning of the tubing due to a 0.75 mm tube insertion socket. The socket simplifies the joint setting process by ensuring consistent and precise alignment of the tubes. Once inserted (figure 4) the inner diameter of the fitting is identical to the base tubes enabling unconstricted coolant mass flow. The fitting consists of the socket ends followed by a thicker section before a return to a thinner central region. This specific shape is to enable accommodation of O-rings to seal connections for quality assurance testing equipment. There is also an additional benefit of the thinner central region — it allows for a standard purchase point for setting the cooling manifolds in a jig during production. With larger diameter tubes, the varying gravitational effect on the weld pool as different regions of the tube are welded can affect the geometry of the weld seam. However, in the present application, the low amperages used and the small size of the weld pool (1–2 mm wide) mean that this does not need to be considered. Using this custom enveloping fitting adds unavoidable mass to the cooling circuit. However, this is a necessary trade-off for production and the increased wall thickness adds additional reliability.

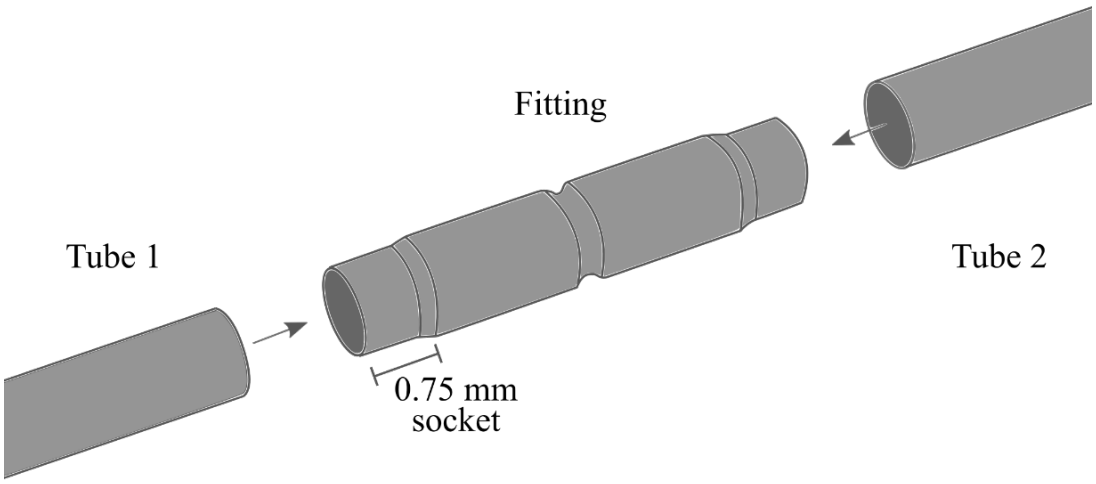

Figure 3. Illustration of the sleeve fitting and socket insertion mechanism for joining two tubes.

3.3 Weld optimization strategy

The welding parameters in GTAW are strongly coupled thus optimizing a GTAW process is complex. Whilst sophisticated mathematical methods may elucidate the effects of different weld parameters, the present work advocates that the application of operator experience and knowledge also provides an efficient strategy for joint optimization. Conventional mathematical optimization for welding procedures necessitates a rigorous focus on the weighted effect of each parameter. Yet, due to the application of the present work, the specific dimensions and geometry of the tubing is subject

2020 JINST 15 P06022

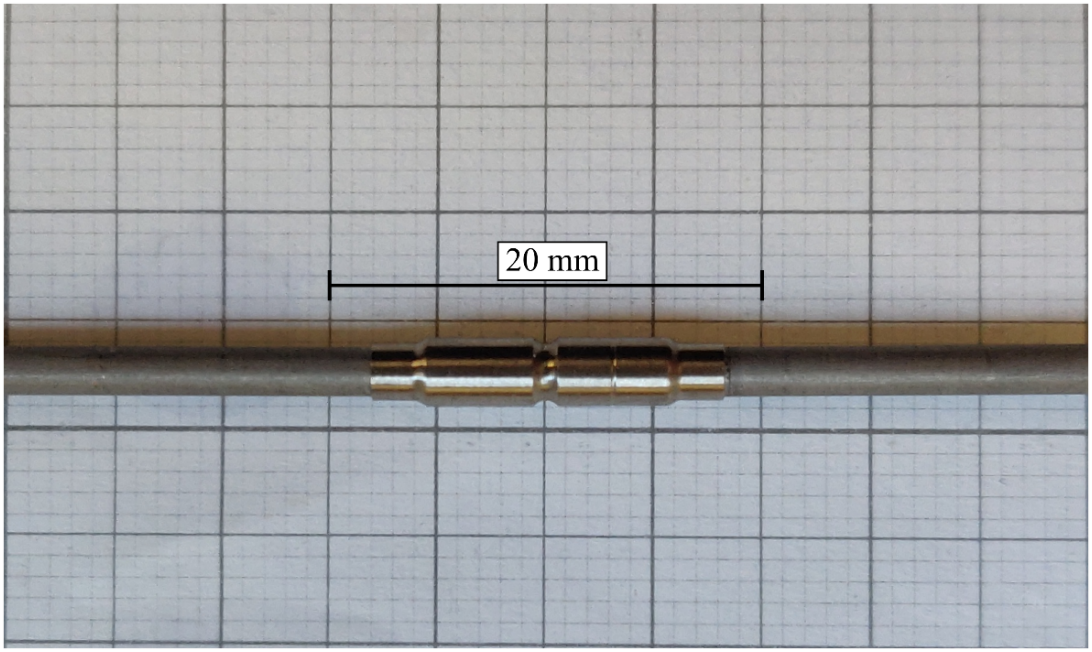

Figure 4. Photo of a sleeve fitting with two tubes inserted.

to change. The cooling circuits form a component within a larger cooling plant assembly. Thus, design changes within the rest of the cooling system of the ITk could make mathematical based optimization of specific joinery scenarios obsolete. Conversely, the application of sound welding principles enables flexibility of a procedure to adapt to design changes. This is particularly acute in the present application due to the incorporation of the sleeve, as it has considerably more mass than the tube and thus the input heat has more material to heat and more neighbouring metal to conduct through. Secondly, the inner pressurization is of less importance in the sleeve area as the molten metal can better support itself. This sleeve-tube interface complicates the parameter interaction significantly from a mathematical optimization perspective. However, a skilled operator can identify the tuning required of individual parameters despite the complex weld situation. For instance, controlling the rotational head speed is vital in preventing porosity within the welds; slowing the travel speed of the rotational head helps eliminate porosity irrespective of the other parameters. The process parameters and effects in this study are shown in table 2.

An initial procedure is required as a basis for parameter optimization. Due to the specificity of the application, the initial procedure was merely an order of magnitude estimation using standard parameter development methodology and reference manuals [35–37]. For instance, a starting point for current is 1 A for every thousandth of an inch so a 160 µm thick work piece equates to around 6.3 A. After an initial procedure is executed, visual inspection is applied to judge the quality of the joint. Through applying visual inspection and adjusting the relevant parameters the welding procedure is optimized. This optimization process combined with the accommodation of changes to the design required approximately 300 welds to complete.

For a skilled operator, visual inspection is an acutely effective assessment method of the effects of individual parameters. For instance, the anatase and rutile (TiO_2) surface formations that occur when shielding gas coverage is insufficient and the bulbous or shrunken tube exterior

2020 JINST 15 P06022

Table 2. Welding parameter definitions.

Welding parameter	Definition and effect
Arc gap	Governs the distance between the electrode tip and work metal along the *z-axis* which, as GTAW is a constant current process, dictates the electrical voltage during welding. In general, a larger voltage results in more heat input.
Main current	Controls the peak current of the InterPulse arc which changes between Main and Interbackground current. Larger currents input more heat into the work metal.
Interbackground current	Controls the background current of the Interpulse arc.
Rotational head speed	Determines the travel speed of the arc around the work metal in a clockwise rotation around the *y-axis*. Together with current and voltage, this parameter determines the heat input. A high rotational head speed can cause porosity due to solidification occurring before gases can escape.
Initial current	Controls the current amperage used when the arc is generated. A large initial current can potentially damage the thin walls of the tubing.
Machine gas flow rate	Controls the amount of shielding gas that engulfs the outside of the work metal. The main role of this flow is to remove impurities from the weld, excessive gas flow can result in arc strike failures.
Internal gas flow rate	Controls the amount of shielding gas that flows inside of the CP-2 Ti tube thereby determining the internal gas pressure at the joint. Precise control is required to ensure consistent internal diameter in the cooling tubes with high flow risking outer blowout and low flow risking inner collapse.
Electrode position	Controls the *y-axis* position of the arc along the work metal, thus determining the location of the heat input.
Socket depth	Controls how far the tube sits within the fitting. Together with the electrode position, the socket depth is essential in positioning the weld bead in the optimum position for the strongest joint. Whilst it is crucial to limit the HAZ, the weld bead needs to be sufficiently large to achieve full fusion between the tube and the sleeve.

2020 JINST 15 P06022

which materializes with inappropriate inner pressurization are two parameters that can be assessed effectively. A key point with visual inspection is that whilst techniques such as Energy Dispersive X-Ray Spectroscopy (EDXS) can give more details on the content of impurities through investigation into discoloration, they effectively match the rejection judgments of a skilled operator. In essence, EDXS or other such methods would not accept a weld rejected by a skilled operator. Visual inspection streamlined the research process to enable procedure alteration without subsequent testing required. Further, there exists a wide range of welding parameters that can achieve a high

quality joint; with the goal of this project being to achieve a high quality joint, the absence of a unique solution further validates the manual optimization method.

3.4 Production set up

Illustrated in figure 5, the production set up uses a VBCie IP50 to power a Polysoude UHP 250 torch with a closed chamber orbital weld head attached. The orbital weld head is fitted with a 2.275 mm tube-clamping insert that encloses the joint during welding. The Polysoude torch and weld head measures 225 × 25 × 50 mm at its greatest extent allowing it to fit easily within small spaces for in situ production. Two 99.9999% pure Argon gas bottles are used: one connected to the IP50 to provide external shielding and the other fed into the CP-2 Ti tube through an external manifold to provide shielding and internal pressurization. A pressure gauge connected to the outflow end of the CP-2 Ti tubing measures the outflow pressure from the inner gas.

Ensuring high reliability in produced welds is vital in delivering a long service life for the cooling manifolds. Thus, before welding both the sleeve and tube are cleaned with an abrasive pad and then washed thoroughly in Isopropyl alcohol (IPA). Further, the inner and machine gas supply manifolds use standard Swagelok fittings to reduce the chance of leaks — increasing the operator confidence in gas supply reliability. Finally, the electrodes are regularly replaced (after 15–20 welds) to ensure that the electrode tip profile is consistent. Figure 6 shows a cross sectional view of the welding torch during production illustrating the process parameters: the blue lines are parts of the Polysoude torch head and electrode, the red line represents the 2.275 mm CP-2 Ti tubing and the grey shape shows the custom sleeve with the insertion socket. The final welding procedure is presented in table 3; details on the linearity of parameter tuning is covered in appendix A.

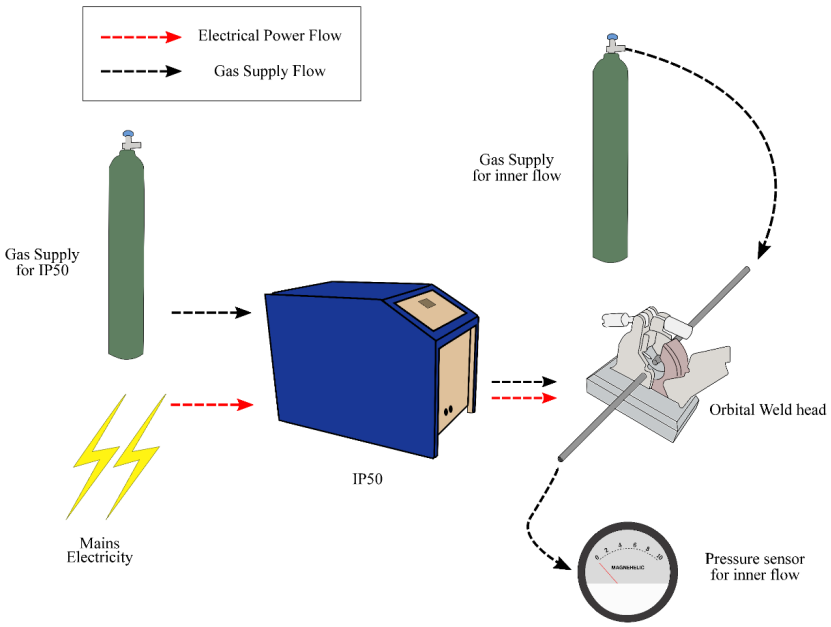

Figure 5. Production set-up showing the electrical power flow and the gas supply.

2020 JINST 15 P06022

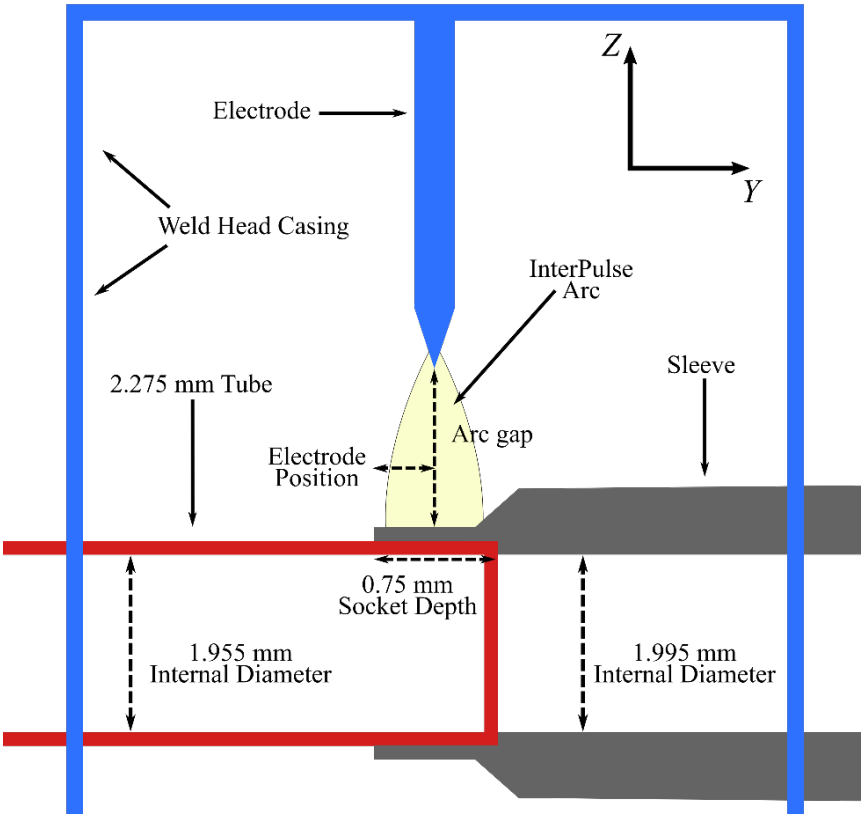

Figure 6. Cross-section view of inside the weld head illustrating the roles of the welding parameters. The blue lines are parts of the Polysoude UHP 250 weldhead and the electrode, the red line represents the CP-2 Ti tubing, and the grey areas show the sleeve fitting.

Table 3. Final procedure welding parameters.

Welding parameter	Value
Arc gap (mm)	0.76
Main current (A)	6.0
Interbackground current (A)	6.8
Rotational head speed (RPM)	25
Initial current (A)	2.40
Machine gas flow rate (l/min)	2.50
Internal gas flow rate (l/min)	4.25
Electrode position (mm)	0.75
Socket depth (mm)	1.00

4 Results

There are several requisite quality criteria to judge the joinery of the CP-2 Ti tubing; ultimate tensile strength, constant internal diameter, absence of gas pores, absence of distortion, complete fusion, leak tightness and minimal heat affected zone. Any gas pore, or an inconsistent internal

2020 JINST 15 P06022

diameter or any lack of fusion qualified as a procedure rejection. The ultimate tensile strength of the weld was required to exceed the base CP-2 Ti material and an excessive HAZ would qualify as a rejected weld. A selection of full mosaic micrographs of acceptable welds on 2.275 mm CP-2 Ti tubing is shown in figure 7. The samples displayed show full fusion, an absence of gas pores and a reasonably constant internal diameter. Whilst both consist of CP-2 Ti, the tube and sleeve are made by different manufacturers and by different processes. This results in differences in the microstructure and mechanical properties in the sleeve and the tube. Thus, to allow for a precise description of the samples, the welded samples can be split into five areas; sleeve base metal, sleeve HAZ, fusion zone, tube HAZ and tube base metal.

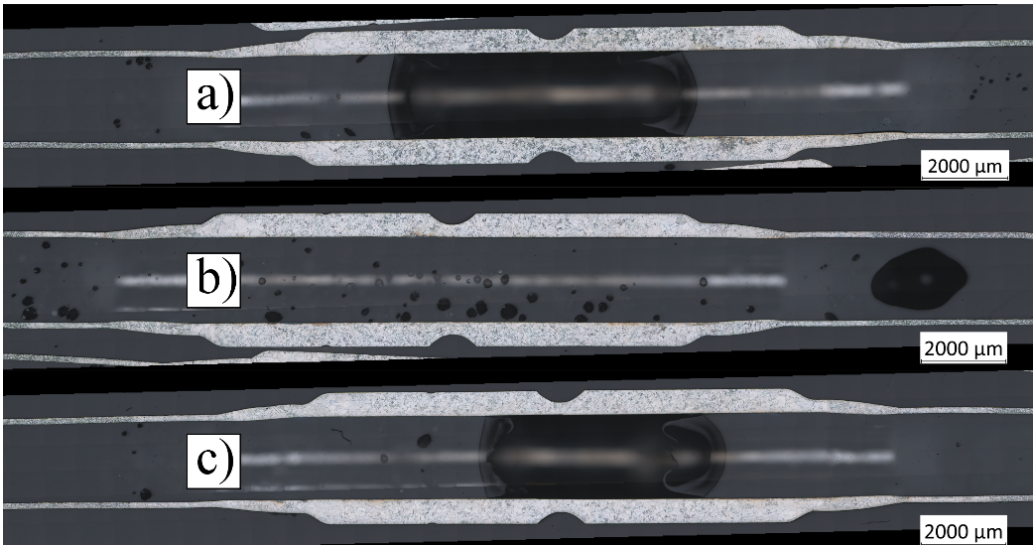

Figure 7. a), b) and c) Mosaic micrographs of full tube-sleeve-tube joints taken under polarized light.

4.1 Mechanical properties

The Ultimate Tensile Strength (UTS) and Total Elongation (TE) of five welded samples were tested with a ZPM machine equipped with a 1 kN load cell. Clamped vertically with pressure grips 35 mm apart, the samples were elongated at 0.5 mm per minute (Method A2 of ISO 6892-1 [38]). As shown in figure 8, the five weld samples have UTS in the 398.0–408.9 range with TE varying between 2.2 and 3.0%. The average UTS of the samples was 403.8 ± 4.2 MPa with an average elongation of 2.5 ± 0.3%. This average exceeds the UTS of the base CP-2 Ti material, 340 MPa [39]. All samples broke in the tube HAZ indicating reasonable weld quality. Ideally, a break in the base metal would be achieved yet the break in the HAZ is still at a larger UTS than the minimum specified UTS of CP-2 Ti validating the procedure. A microhardness survey was carried out under a load of 100 g with a Vickers indenter to assess the hardness throughout the welded CP-2 Ti tubes. Figure 9 shows the hardness profile across the full length of the sleeve-weld-tube regions of a 2.275 mm CP-2 Ti tube sample. Here, the Vickers number (HV) varies between 127.6 (in the tube HAZ) and 218.3 (in the sleeve HAZ). Intrinsic variations in the microstructure account for the fluctuations within each region however, each region exhibits its own hardness characteristics. The martensitic acicular structure in the FZ region accounts for its higher HV matching previous reports [19, 40] of a higher

2020 JINST 15 P06022

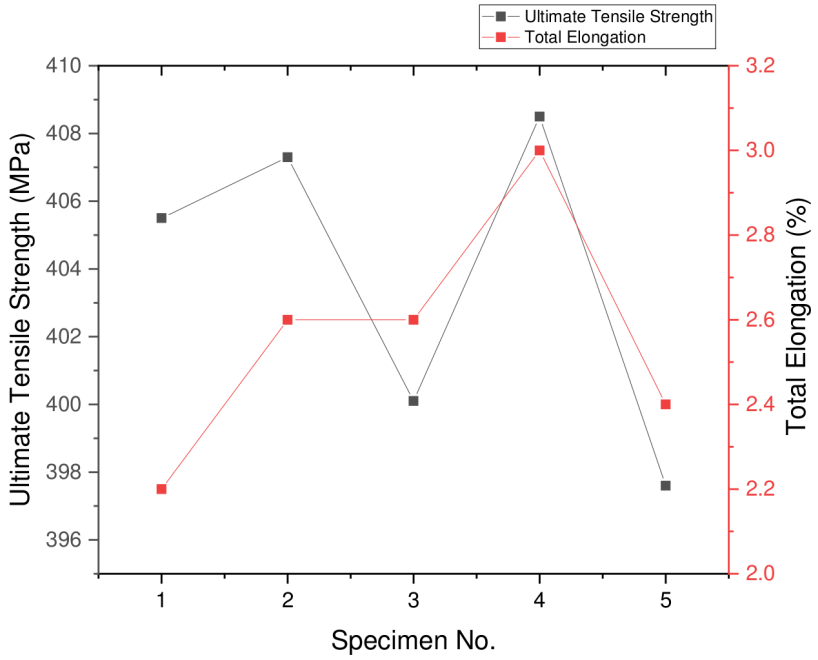

Figure 8. Ultimate Tensile Strength and Total Elongation for five CP-2 Ti tube welds.

HV in the weld FZ compared to BM for GTAW welds of commercially pure titanium. Yet the HAZ in the tube has a noticeable lower HV than the HAZ in the sleeve. As the sleeve and tube are from different manufacturers some variation in the BM hardness is to be expected. The variation in the direction of HV change is due to the manufacturing process; the tubes are cold drawn and the sleeves machined. The cold drawn tubes are effectively in a compressed state that is relaxed by the welding arc heat, whereas, the sleeve does not appear to have any residual stresses with its HAZ with HV variation due variations in α and β phases.

4.2 Microstructural examination

For general microstructural characterization, welded tube-sleeve-tube samples were mounted in cold set resin. Then, the samples were ground down to a longitudinal axis plane with progressively finer grit paper and diamond suspensions before a final polish with colloidal silica suspension and etching with Etchant #192 of ASTM E407 [41]. To illuminate the microstructure, imaging was performed under polarized light. As the tube inserted into a socket within the sleeve and, as the weld is orbital, it is unfeasible to identify the fusion line. The sleeve and tube have different base microstructures; as highlighted in figure 10 the base sleeve has an ASTM Grain size number [42] of 4.5 whereas the tube has a ASTM Grain size number of 8.6 thus the tube has considerably smaller grains than the sleeve. The base metal structure in the sleeve clearly shows a typical equiaxed α titanium microstructure with multiple in-grain dislocations of elongated α microstructure. The structure of the tube base metal is similar except for a noticeably smaller average grain size.

The solid-state transformations in HAZ play a critical importance in weld integrity. As the sleeve and tube have different base metal microstructure, they have different HAZ microstructures. The HAZ in both the sleeve and the tube is shown in figure 11. The HAZ in the sleeve shows

2020 JINST 15 P06022

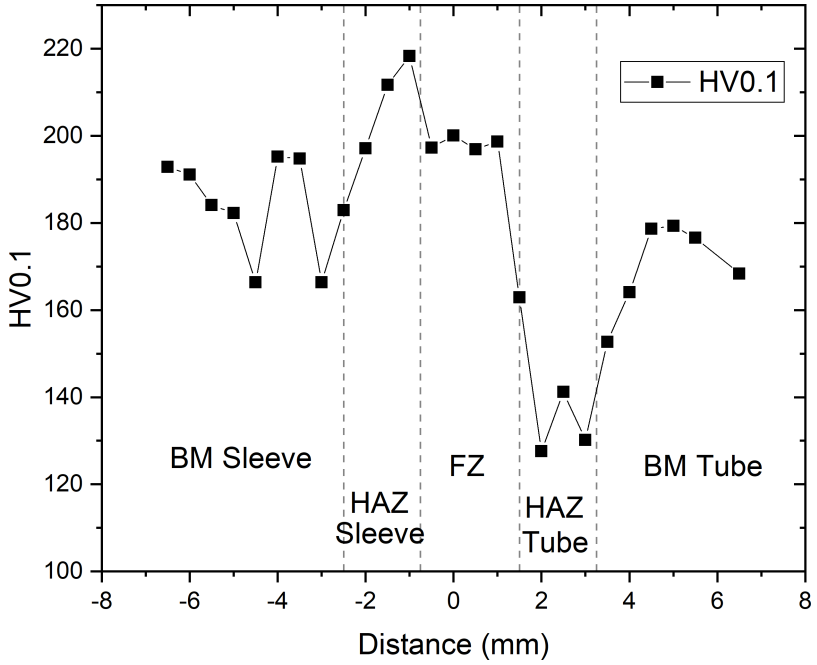

Figure 9. Micro Hardness measurements along the full length of the sleeve-weld-tube for the CP-2 Ti tubing.

increased grain growth reaching an ASTM Grain size number of 3.1 with a noticeable reduction of in-grain dislocations compared to the BM. The HAZ in the tube also shows significant grain growth reaching an ASTM Grain size number of 5.5 whilst also retaining some in-grain dislocations. Predictably, both HAZ regions exhibit decreasingly coarse grains at an increased distance from the fusion zone. A micrograph of the fusion zone is shown in figure 12 displaying complete fusion of the tube and sleeve. Typically, the grain size in the fusion zone of a weld is the largest due to the longest dwell time at elevated temperatures which is exacerbated by the relatively low thermal conductivity of CP-2 Ti (16.4 $Wm^{-1}K^{-1}$). However, in the present work with the thin walls of the tube, the complex heat flow in orbital welding, the difference in grain sizes of the base metal and, the GTCAW process used, the grain size in the weld does not exceed that of the larger sleeve grain size instead manifesting as acicular α phase structure. This acicular structure is typical of a higher cooling rate despite the longer dwell time at the elevated temperatures used in this process.

4.3 Acceptable joint range

Of particular importance in the production of the welded joints was the inner pressure management. Consultation with industrial welding professionals and application of operator knowledge allowed for a manually optimized welding procedure to be established. With a welding procedure that consistently passed visual inspection established, a modified NASA arc welding optimization methodology [43] was applied to the inner pressure management to investigate the range of acceptable inner pressures. Once a base procedure is established, the NASA optimization technique essentially involves performing a minimum of three welds at the nominal procedure then a minimum of three welds at a “limit low” heat input setting and a corresponding three welds at a “limit high” heat input setting. However, in the present application, a sufficient heat input can produce a

2020 JINST 15 P06022

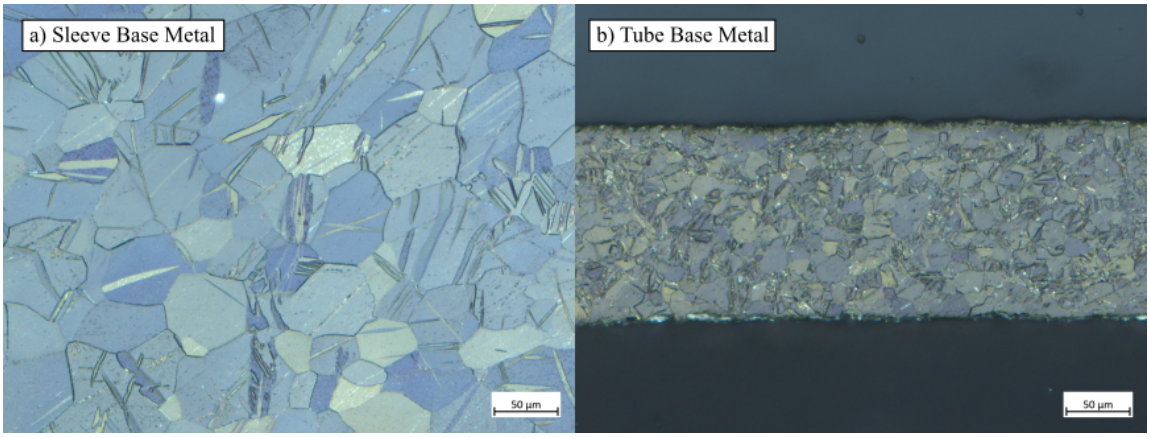

Figure 10. a) Base metal microstructure of the sleeve fitting, b) Base metal microstructure of the tube.

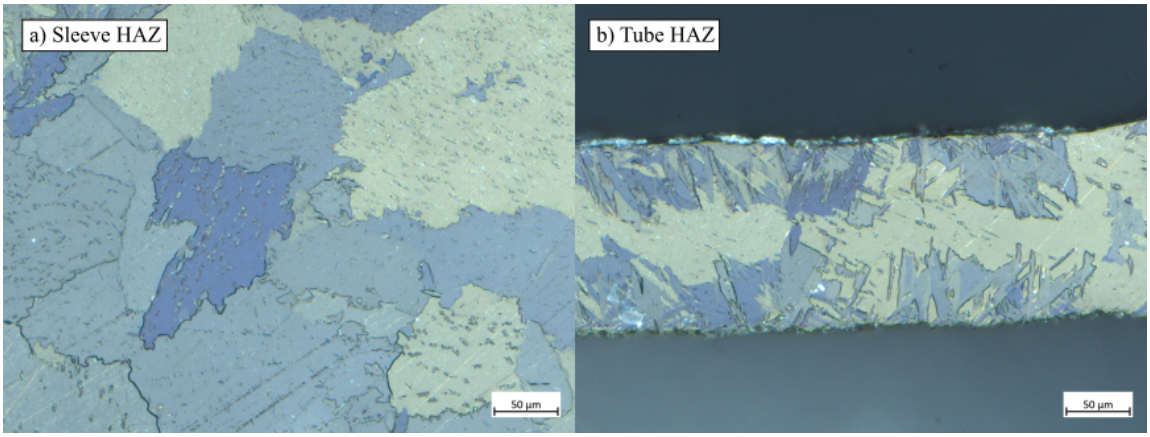

Figure 11. a) Heat affect zone of the sleeve fitting, b) Heat affect zone of the tube, the bright spots on the edges of the sleeve are colloidal silica particles embedded during polishing of the sample.

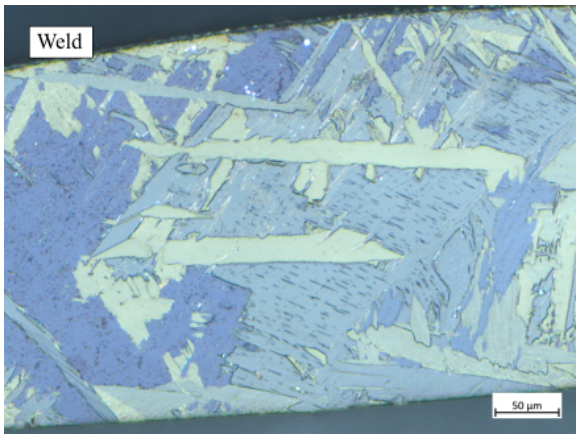

Figure 12. Fusion zone region of weld with acicular grain structure.

2020 JINST 15 P06022

variety of welds depending on the other parameters. Through altering inner gas pressure as well as heat input location, both acceptable and rejected welds can be produced. To assess the range of acceptable inner diameter pressure, the inner gas flow was varied to find the 'limit high' and 'limit low' of the final welding procedure listed in table 3. The low limit was found to be 1194 Pa whereas the high limit was found to be 1742 Pa. Figure 13 shows a selection of the produced welds. Welds 1 and 2 show the lower 'low limit' of inner pressure; whilst Weld 1 nearly buckled but successfully fused, Weld 2 completely collapsed due to the insufficient gas pressure. This shows 1194 Pa to be the effective low limit. Welds 3 and 4 are with an ideal procedure and an inner diameter pressure of 1448 Pa displaying excellent exteriors. In Welds 5 and 6 the inner gas pressure is increased beyond the acceptable range showing bulging as the gas pressure pushes the molten metal out. These results

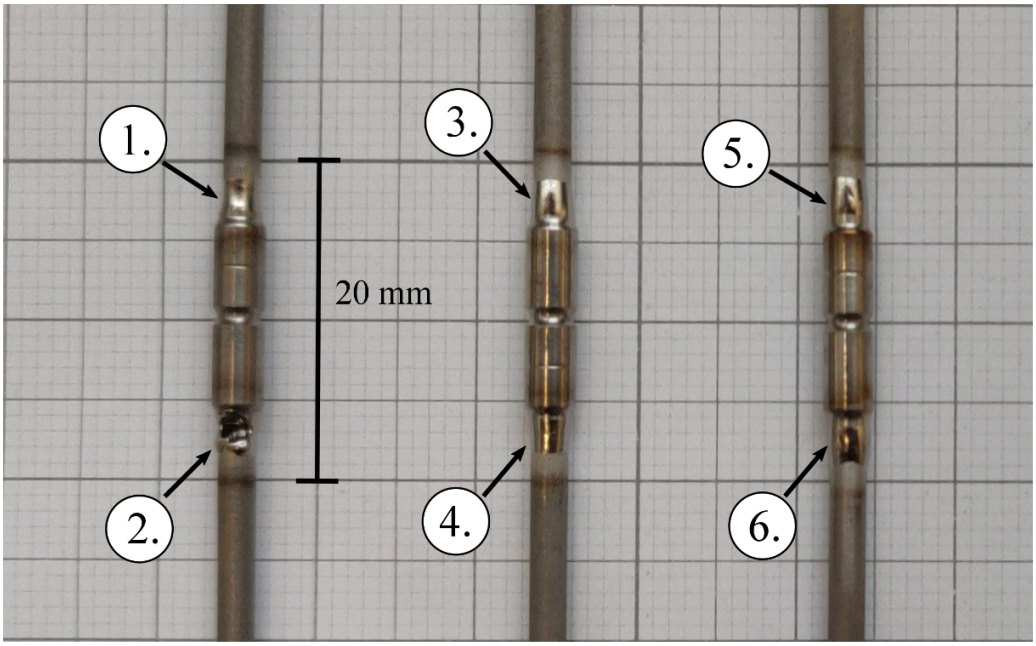

Figure 13. Photograph of a selection of welds with 'low limit' inner diameter pressurization (1,2), correct inner diameter pressurization (3,4) and 'high limit' inner diameter pressurization (5,6).

raise interesting questions about the parameter balance of the inner pressure. The force pushing the weld inwards against the inner pressure is the stagnation pressure from the impinging plasma arc. The clear difference in microstructure of the fusion zone compared to the HAZ and base metal (covered in section 4.2) indicate that the weld penetrated through the entire wall thickness. This suggests that during the welding process a liquid metal disk is suspended between the two competing forces. As the pressure from GTAW arcs peaks in the centre of the arc it therefore follows that this liquid metal disk is subject to a Laplace pressure as it curves to accommodate the competing pressures. However, an order of magnitude estimation of the pressure from a conventional GTAW arc at the current levels used [44] indicate that the arc pressure is considerably less than the inner pressurization. Similarly, the magnitude of gravity is not significant enough (relative to surface tension and inner pressurization) to affect this pressure balance. One explanation for this is that due to the orbital arc, the liquid metal disk could solidify before it has chance to collapse — termed a kinematics issue. However, determining this requires accurate measurements of the heat input

2020 JINST 15 P06022

from the InterPulse arc to assess the melting and solidification time. Another explanation would be that the pressures of GTCAW are considerably different to conventional GTAW indicating that this issue is a pressure equalization problem. It is not clear whether this is a kinematics problem or a pressure equalization problem. This issue is currently the subject of further study.

4.4 Cooling circuit production

The joinery method outlined in section 3 was applied to a cooling circuit exhaust manifold, shown in figure 1. The cooling circuit exhaust manifold consists of a vacuum brazed manifold head with eight "legs" that are individually welded to separate cooling tubes. The end of the vacuum brazed manifold head is the main outlet from which the coolant leaves the cooling circuits. The complex curving geometry of the cooling circuit means the required gas inlet flow for an apt inner diameter pressure changes for each weld. The solution to this is to initially flow the gas through just the manifold head to find the required inlet flow for the correct inner pressure at the weld (the other legs in the manifold are blocked off so that the only outlet is the point of weld). With the required inflow to achieve the correct inner pressure at the weld established, the legs are attached and the pressure measured at the new outlet (the end of the tube leg). A tube socketed in the sleeve pre-welding has the same pressure handling ability as when post-welded (see appendix B). Therefore, repeat construction of the identical manifolds will only require the outflow from the leg to be measured to ensure consistency as the required inflow has already been identified. This is important for the in situ application where gas flow may be more challenging to measure. Close up images on some of the manifold welds are shown in figure 14.

The particular challenge in welding this cooling circuit is the fixed geometrical orientation of the tubes. In the previous work by the authors [13, 14], the joints required re-orientation to match the imperfect ends of the tubes together yet the specific angles required for this cooling circuit means that re-orientation is not an option. The incorporation of the sleeve fitting negates the need for re-orientation and aids joint setting. This cooling circuit will be used in a mock up cooling plant for the forthcoming ATLAS ITk. This demonstrates the industrial viability of this method as the cooling circuit is genuine. Due to the small size of the orbital weld head, the joinery technique can be performed in situ in a variety of environments. As this cooling circuit is a final product, destructive tests are not apt but the high repeatability in the welding process combined with visual inspection leads to confidence in the product.

5 Discussion

In this paper, we have demonstrated that for production, a sleeve fitting enhances the joinery of ultra-thin walled tubes allowing joint setting in fixed geometry parts and, excluding inner gas flow rate, a consistent welding procedure to apply to all joints. The principle advantage of the sleeve fitting is the added reliability; thin-walled tubes are particularly challenging to join and whilst tube-to-tube butt joinery is feasible to perform in a lab environment, the transfer into industrial production greatly benefits from the inclusion of the sleeve. This sleeve thus serves as an improvement compared to butt joints of thin-walled tubes and is successfully demonstrated on thinner-walled tubing than reported previously [8]. Reliability is the main challenge when welding thin-walled tubing; many welding machines are not optimized for the required low amperages of thin-walled tube welding so

2020 JINST 15 P06022

Figure 14. Photographs of welds from the demonstration ATLAS ITK cooling circuit manifold.

welding procedures are awkward to translate between different machines. Thus, process additions that enhance the reliability of production are highly valuable.

The substantial pre and post weld gas flow used is constructive to reliable welds supporting previous work on shielding gas flow when welding CP titanium [17–19]. As the required inner diameter pressurization used is so low, small leaks in the gas supply system can result in failed welds. This inner pressure management is vital in producing a quality weld in a complex manifold. This is achieved through the tuning of the gas inlet flow. When the manifold can be separated this is relatively straightforward to perform. However, should the manifold already be integrated into a larger system, as will be the case for the full production of the ATLAS upgrade, this is more challenging to perform. A possible solution to this is to use computational fluid dynamics (CFD) to calculate the gas flow throughout the manifold to identify the required inlet flow to achieve the correct inner pressure for any particular weld. However, there are several challenges in using CFD to find the required inlet flow. Principally, due to the complex geometry of the manifold there is not an analytical solution to the Navier-Stokes equations available. Thus, the required inlet flow would have to be found through simulation for each individual weld within a manifold. Secondly, matching a theoretical gas delivery to a physical system with unanticipated leaks is challenging. This second point illustrates the greater practical value of manually tuning the gas flow and measuring it as close to the weld as is feasible compared to finding the required flow through CFD simulations. Ultimately, it is the physical conditions during welding that determine weld quality and therefore it is more productive to focus on practical measurements.

6 Conclusion

The present work outlines a full procedure for joinery of fixed geometry ultra-thin-walled titanium tubing for the ATLAS ITk Strip Detector staves, addressing the paucity of research on ultra-thin-walled tube joinery. The procedure maintains a consistent inner diameter throughout the weld,

2020 JINST 15 P06022

which ensures consistent mass flow in the cooling system. The sleeve fitting presented greatly improves the joint setting capabilities in the ultra-thin-walled tubes facilitating joinery on fixed geometry parts. Additionally, the work demonstrates how manual optimization performed with skilled operator knowledge can achieve quality joints in a complex multi-response system. When welding parameter interaction is intuitively understood, and parameter interaction strength variable, the application of sound welding principles can create novel joinery procedures without the need for sophisticated mathematical methods. Finally, the work highlights how inner pressure management is key in ensuring production of acceptable welds in thin-walled tubing. With the inclusion of the sleeve fitting, the pressure handling ability of the mechanical joints match that of the welded joints. This aids in determining the required gas inlet flow during production. CFD simulation of the correct flowrate for the required inner diameter pressure is challenging and manual testing is shown to be sufficient to identify the required flowrate. It is unclear whether achieving apt inner pressurization is a kinematics or a pressure balance issue, this is currently the subject of further study.

The implications of this work are a validation of GTCAW with inner gas flow for thin-walled tube joinery as a practicable method. With this method shown to be feasible, and to work for a deployable manifold, the industrial applicability is clear. Small diameter thin-walled tubing used in high-value-added industries such as aerospace can apply this joinery method. Thus, this work stands as an example in an area with limited previous work.

Acknowledgments

We acknowledge the support of UK-ATLAS, STFC, EPSRC, INNOVATE-UK and VBC Instrument Engineering. Additionally, the authors are grateful to the following individuals from The University of Sheffield; Tesoro Monaghan from the Department of Materials Science, Razvan Apetrei from the Department of Mechanical Engineering, Heather Grievson from the Department of Chemistry and Toby Dowling from the Department of Physics and Astronomy, for their help and invaluable support.

A Linearity of current setting to output

A predictable response to parameter changes allows for operator confidence when optimizing the welding procedure. The Insulated-Gate Bipolar Transistors (IGBTs) in many welding power supplies do not provide a linear output at particularly low current levels. Whilst IP50 is optimized specifically for low currents a quality assurance test was performed to ensure the output current was equal to the current the machine was set to. The current was set to a variety of amplitudes between four and eight amperages and the output current was measured with a custom-built shunt box with two additional repeats performed. Figure 15 shows the strong linear correlation between the set current compared to the output current — thus confidence that the current output of the IP50 varies linearly is established. Similarly, ensuring a linear increase of inner pressurization with an increase in gas flow enables confidence when tuning the internal gas pressure. Figure 16 shows this to be true. Of note is the challenge in production consistency; the gas flow manifold demanded regular inspection to ensure consistent flow rate.

2020 JINST 15 P06022

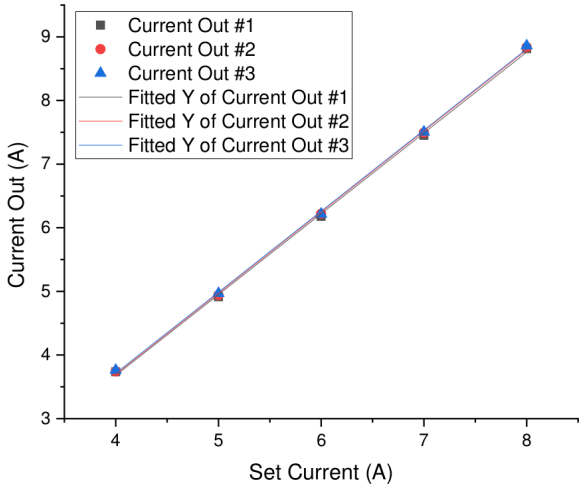

Figure 15. Visualization of current linearity showing current the welding machine is set to (set current) vs output current measured with a custom shunt box.

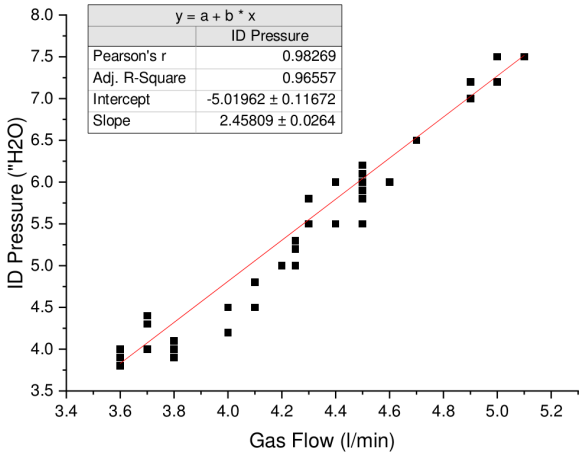

Figure 16. Inner diameter pressure in inches of water vs gas flow in litres per minute.

B Cooling circuit production

The pressure handling abilities of the mechanical joints (the tube inserted into the sleeve socket with no additional processing) and the welded joints are strongly correlated. Measurements taken on 310 welds show the inner gas pressure pre-welding is typically equal to the inner gas pressure post-welding. Figure 17 shows the strength of the correlation.

References

[1] ATLAS collaboration, *The ATLAS Experiment at the CERN Large Hadron Collider*, 2008 *JINST* **3** S08003.

[2] ATLAS collaboration, *ATLAS Phase-II Upgrade Scoping Document*, CERN-LHCC-2015-020 (ATLAS Phase-II Upgrade Scoping Document).

2020 JINST 15 P06022

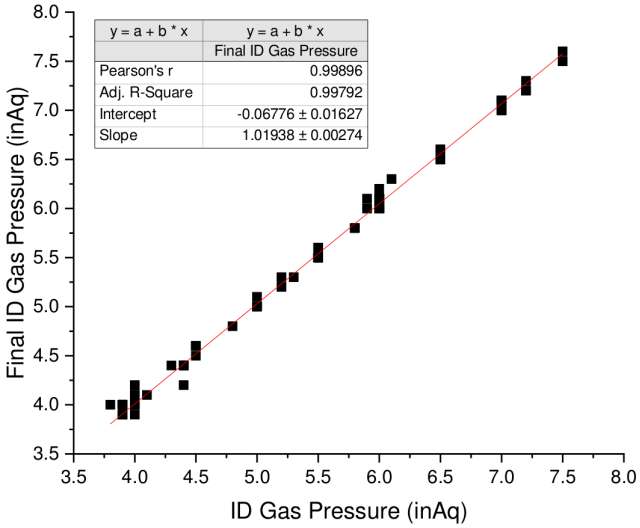

Figure 17. Inner gas pressure pre-weld (ID Gas Pressure) vs Inner gas pressure post-weld (Final ID Gas Pressure) for 310 welds. Many welds were performed at the same inner gas pressure leading to redundancy in data points.

[3] ATLAS collaboration, *Technical Design Report for the ATLAS Inner Tracker Strip Detector*, CERN-LHCC-2017-005 (Technical Design Report for the ATLAS Inner Tracker Strip Detector).

[4] ASTM, *Standard Specification for Titanium and Titanium Alloy Welded Pipe*, B862-14 (2014).

[5] ASME, *Standard Specification for Titanium and Titanium Alloy Welded Pipe*, SB-862 (2014).

[6] ASTM, *Standard Specification for Seamless and Welded Titanium and Titanium Alloy Condenser and Heat Exchanger Tubes*, B338-17 (2017).

[7] Q. Yunlian, D. Ju, H. Quan and Z. Liying, *Electron beam welding, laser beam welding and gas tungsten arc welding of titanium sheet*, *Mater. Sci. Eng.* **A 280** (2000) 177.

[8] J.A.O. de Garcia, N.S. Dias, G.L. de Lima, W.D.B. Pereira and N.F. Nogueira, *Advances of orbital gas tungsten arc welding for Brazilian space applications — Experimental setup*, *J. Aerosp. Technol. Manag.* **2** (2010) 211.

[9] Y. Miyamoto, T. Nishimura, Y. Fukuhara, Y. Koyama, K. Narita And E. Sawahisa, *Production of thin wall welded titanium tubes by high frequency pulsed arc welding*, *Trans. Iron Steel Inst. Jap.* **26** (1986) 484.

[10] S. Carvalho, C. Baptista and M. Lima, *Fatigue in laser welded titanium tubes intended for use in aircraft pneumatic systems*, *Int. J. Fatigue* **90** (2016) 47.

[11] A. Kumar, M. Sapp, J. Vincelli and M.C. Gupta, *A study on laser cleaning and pulsed gas tungsten arc welding of Ti-3Al-2.5V alloy tubes*, *J. Mater. Process. Technol.* **210** (2010) 64.

[12] R.K. Leary, E. Merson, K. Birmingham, D. Harvey and R. Brydson, *Microstructural and microtextural analysis of InterPulse GTCAW welds in Cp-Ti and Ti-6Al-4V*, *Mater. Sci. Eng.* **A 527** (2010) 7694.

[13] R. French and H. Marin-Reyes, *Investigation of the TIG orbital welding process on tube-to-tube joints in titanium & stainless steel thin wall tubes*, in proceedings of the *68th IIW Annual Assembly High-Strength Materials — Challenges and Applications*, Helsinki, Finland, 2–3 July 2015.

2020 JINST 15 P06022

[14] R. French and H. Marin-Reyes, *Welding performance evaluation of the VBC instrument engineering IP50 TIG orbital heat management system*, in proceedings of the *68th IIW Annual Assembly High-Strength Materials — Challenges and Applications*, Helsinki, Finland, 2–3 July 2015.

[15] R. Wang and G. Welsch, *Joining titanium materials with tungsten inert gas welding, laser welding, and infrared brazing*, *J. Prosthet. Dent.* **74** (1995) 521.

[16] M.S. Oh, J.-Y. Lee and J.K. Park, *Continuous cooling β-to-α transformation behaviors of extra-pure and commercially pure Ti*, *Metall. Mater. Trans.* **A 35** (2004) 3071.

[17] A. Karpagaraj, N. Siva Shanmugam and K. Sankaranarayanasamy, *Experimental investigations and numerical prediction on the effect of shielding area and post flow time in the GTAW of CP Ti sheets*, *Int. J. Adv. Manuf. Technol.* **101** (2018) 2933.

[18] Winarto, M. Anis and M. Laili Solichin, *Influence of shielding gas on the mechanical properties and visual surface of the welded cp titanium*, *Weld. World* **53** (2009) 523.

[19] R. Bendikiene, S. Baskutis, J. Baskutiene, A. Ciuplys and T. Kacinskas, *Comparative study of TIG welded commercially pure titanium*, *J. Manuf. Process.* **36** (2018) 155.

[20] K.K. Murthy and S. Sundaresan, *Phase transformations in a welded near-α titanium as a function of weld cooling rate and post-weld heat treatment conditions*, *J. Mater. Sci.* **33** (1998) 817.

[21] S.K. Kim and J.K. Park, *In-situ measurement of continuous cooling $\beta \rightarrow \alpha$ transformation behavior of CP-Ti*, *Metall. Mater. Trans.* **A 33** (2002) 1051.

[22] I. Lonardelli, N. Gey, H.-R. Wenk, M. Humbert, S. Vogel and L. Lutterotti, *In situ observation of texture evolution during $\alpha \rightarrow \beta$ and $\beta \rightarrow \alpha$ phase transformations in titanium alloys investigated by neutron diffraction*, *Acta Mater.* **55** (2007) 5718.

[23] A.B. Murphy, *A perspective on arc welding research: The importance of the Arc, unresolved questions and future directions*, *Plasma Chem. Plasma Process.* **35** (2015) 471.

[24] E.A. Bel'skaya and E.Y. Kulyamina, *Electrical resistivity of titanium in the temperature range from 290 to 1800 K*, *High Temp.* **45** (2007) 785.

[25] M. Yousefieh, M. Shamanian and A. Saatchi, *Influence of heat input in pulsed current GTAW process on microstructure and corrosion resistance of duplex stainless steel welds*, *J. Iron Steel Res. Int.* **18** (2011) 65.

[26] A. Traidia and F. Roger, *Numerical and experimental study of arc and weld pool behaviour for pulsed current GTA welding*, *Int. J. Heat Mass Transf.* **54** (2011) 2163.

[27] M. Balasubramanian, V. Jayabalan and V. Balasubramanian, *Response surface approach to optimize the pulsed current gas tungsten arc welding parameters of Ti-6Al-4V titanium alloy*, *Met. Mater. Int.* **13** (2007) 335.

[28] M. Balasubramanian, V. Jayabalan and V. Balasubramanian, *Effect of process parameters of pulsed current tungsten inert gas welding on weld pool geometry of titanium welds*, *Acta Metall. Sin. (English Lett.)* **23** (2010) 312.

[29] N.K. Babu and S.G.S. Raman, *Influence of current pulsing on microstructure and mechanical properties of ti–6al–4v TIG weldments*, *Sci. Technol. Weld. Joining* **11** (2006) 442.

[30] C.L. Tsai and C.A. Hou, *Theoretical analysis of weld pool behavior in the pulsed current GTAW process*, *J. Heat Transfer* **110** (1988) 160.

[31] H. Saedi and W. Unkel, *Arc and Weld Pool Behavior for Pulsed Current GTAW High-frequency current pulsing can be used to control the geometry of a GTA weld pool*, *Weld. J.* (1988) 247s.

2020 JINST 15 P06022

[32] M. Yang, B. Qi, B. Cong, F. Liu, Z. Yang and P.K. Chu, *Study on electromagnetic force in arc plasma with UHFP-GTAW of Ti-6Al-4V*, *IEEE Trans. Plasma Sci.* **41** (2013) 2561.

[33] B.J. Qi, M.X. Yang, B.Q. Cong and F.J. Liu, *The effect of arc behavior on weld geometry by high-frequency pulse GTAW process with 0cr18ni9ti stainless steel*, *Int. J. Adv. Manuf. Technol.* **66** (2012) 1545.

[34] M. Yang, H. Zheng and L. Li, *Arc shape characteristics with ultra-high-frequency pulsed arc welding*, *Appl. Sci.* **7** (2017) 45.

[35] B. Mannion and J. Heinzman, *Setting up and determining Parameters for Orbital Tube Welding*, https://www.pro-fusiononline.com/pdf/fab-may99.pdf (1999).

[36] B. Mannion and J. Heinzman, *Determining parameters for GTAW*, *Pract. Weld. Today* (1999).

[37] Swagelok *M200 Power Supply User's Manual*, (2007).

[38] ISO 6892-1:2019, *Metallic materials — Tensile testing — Part 1: Method of test at room temperature*.

[39] A. Mouritz, *Titanium alloys for aerospace structures and engines*, in *Introduction to Aerospace Materials*, Elsevier, (2012), pp. 202–223, DOI.

[40] A. Karpagaraj, N. Siva Shanmugam and K. Sankaranarayanasamy, *Some studies on mechanical properties and microstructural characterization of automated TIG welding of thin commercially pure titanium sheets*, *Mater. Sci. Eng.* **A 640** (2015) 180.

[41] ASTM, *E407-07 Standard Practice for Microetching Metals and Alloys*, (2012).

[42] ASTM, *E112-13: Standard test methods for determining average grain size*, (2013).

[43] NASA, *Process Specification for Automatic and Machine Arc Welding of Steel and Nickel Alloy Hardware*, *NASA Eng. Dir.* (2012) 1–29.

[44] M.L. Lin and T.W. Eagar, *Pressures produced by gas tungsten arcs*, *Metall. Trans.* **B 17** (1986) 601.

2020 JINST 15 P06022